Supporting Information for:

Graphene-Ni-α-MnO_2 and -Cu-α-MnO_2 nanowire blends as highly active non-precious metal catalysts for the oxygen reduction reaction

Timothy N. Lambert,*[a] Danae J. Davis,[a] Wei Lu,[b] Steven Limmer,[c] Paul Kotula,[d] Alexis Thuli,[a] Madalyn Hungate,[a] Gedeng Ruan,[b] Zhong Jin,[b] and James M. Tour*[b]

†Sandia National Laboratories, Albuquerque, New Mexico, 87185

[a] *Department of Materials, Devices & Energy Technologies, Sandia National Laboratories, Albuquerque, New Mexico, 87185, USA, Fax: 505 844 7786; Tel: 505 284 6967; E-mail: tnlambe@sandia.gov,*

[b] *Departments of Chemistry and Mechanical Engineering and Materials Science and the Smalley Institute for Nanoscale Science and Technology, Rice University, Houston, Texas, 77005, Fax: 713 348 6250; Tel: 713 348 6246; E-mail: tour@rice.edu*

[c]*Department of Photonic Microsystems Technology,*
Sandia National Laboratories, Albuquerque, New Mexico, 87185, USA,

[d]*Department of Materials Characterization,*
Sandia National Laboratories, Albuquerque, New Mexico, 87185, USA,

*Author(s) to whom correspondences should be sent

Synthesis of α-MnO_2 nanowires[1, 2]

A solution of $MnSO_4 \cdot H_2O$ (0.2 g, 1.18 mmol) and $KMnO_4$ (0.5 g, 3.16 mmol) in de-ionized water (18 mL) was heated in an acid digestion bomb (Teflon liner, Parr™) at 140 ºC, for either 12 h (to yield nanoflower/nanosphere morphology) or ~ 88 h (to yield nanowire morphology exclusively). The reaction was allowed to cool to rt and the obtained solid was washed with DI H_2O (~4 x 25 mL) and ethanol (~ 1 x 25 mL), and dried *in vacuo*. Ni-α-MnO_2 and Cu-α-MnO_2 materials were achieved with the addition of a nitrate salt precursor [$Ni(NO_3)_2 \cdot 6H_2O$ or $Cu(NO_3)_2 \cdot 3H_2O$] into the previously described reaction solution at initial (molar) ratios of 1:1 (manganese:dopant cation).

Materials Characterization

Powder X-ray Diffraction (PXRD). Powders were mounted directly onto a zero background holder purchased from The Gem Dugout. Samples were scanned at a rate of 0.02°/2 s in the 2θ range of 10−80° on a Bruker D8 Advance diffractometer in Bragg-Brentano geometry with Cu Kα radiation and a diffracted beam graphite monochromator. Phase identification was determined from the PXRD patterns using Jade 9 Software suite and Joint Committee on Powder Diffraction Standards.

Scanning Electron Microscopy (SEM). The samples were dispersed onto carbon tape and imaged using a Zeiss Supra 55VP field emitter gun scanning electron microscope (FEGSEM). A Noran EDS detector and Noran System Six software were used for the acquisition of the EDS spectra. EDS data was re-plotted with Kaleidagraph for presentation purposes. Samples were sputter coated with gold-palladium prior to analysis.

Brunauer-Emmett-Teller (BET) surface area analysis. N_2 adsorption/desorption on composite samples was measured using a Micrometrics Tristar 3000 sorptometer.

X-ray photoelectron spectroscopy. X-ray photoelectron spectroscopy (XPS) was performed with a Kratos Axis Ultra DLD with monochromatic Al Kα (1486.6 eV) source at 225 W, and an analyzer pass energy of 20 eV. The analyzed spot size was 300 x 700 microns and base pressures were less than 5 x 10^{-9} Torr. Charge neutralization was used for all samples. Data were analyzed using CasaXPS software. Peaks were fit using a Shirley background and a Gaussian/Lorentzian line shape.

Scanning Transmission Electron Microscopy (STEM). The nanowire samples were dispersed in isopropanol and dropped onto carbon coated aluminium grids, allowed to dry and analysed. An FEI Company Titan G2 80-200 with ChemiSTEM technology was operated at 200kV and equipped with a bright electron source, probe spherical aberration corrector and four-silicon-drift x-ray detector array integral to the objective lens. This system is capable of structural and chemical analysis down to sub-Angstrom dimensions for imaging and the ability to perform x-ray microanalysis and

quantification at atomic resolution. The hyperspectral x-ray data acquired with this instrument at sub-nm resolution were analyzed with Sandia's Automated eXpert Spectral Image Analysis (AXSIA) software whereby the entire data set is subjected to multivariate statistical analysis algorithms capable of discerning subtle elemental inhomogeneities without prior knowledge. For further information please refer to: Kotula, P.G., Keenan, M.R. & Michael, J.R. (2003). Automated analysis of EDS spectral images in the SEM: A powerful new microanalysis technique. Microsc Microanal 9, 1–17. Kotula, P.G. & Keenan, M.R. (2006). "Application of Multivariate Statistical Analysis to STEM X-ray Spectral Images: Interfacial Analysis in Microelectronics." Microsc. Microanal. 12, 538–544.

Electrochemistry Measurements

Cyclic voltammetry and rotating disk electrode (RDE) studies were performed on a VoltaLab RDS010 Rotating Disk Stand controlled by a VoltaLab PGZ100 All-In-One Potentiostat as follows: The working electrode was composed of a rotating disk electrode (RDE) with glassy carbon (GC) substrate (d = 5 mm, 0.1963 cm^2). Prior to each use, the GC electrode surface was polished with alumina slurry and rinsed thoroughly with deionized water. A known amount of the synthesized material (α-MnO_2, Ni-α-MnO_2, Cu-α-MnO_2, or carbon blend thereof) was deposited on the electrode as an aliquot of homogenously dispersed "ink." Ink solutions were prepared as follows: 10 mg of the material was dispersed in isopropanol (400 µL) with sonication and then Nafion solution (600 µL, 5% by wt.) was added. This suspension was placed back into the bath sonicator (~ 30 min) to form a well-dispersed, ink-like solution. Immediately following, 10 µL of the ink was pipetted onto the GC surface and then allowed to air-dry.

A three-electrode cell was assembled; the counter was Pt^o and a Hg/HgO electrode (0.1 M KOH) served as the reference (nominal potential of 0.171 V versus a standard hydrogen electrode). The previously described electrode served as the working electrode. The electrolyte was 0.1 M KOH solution, purged with either O_2 or N_2 (for background subtraction). The appropriate gaseous atmosphere was maintained throughout experimentation. Linear scanning voltammograms were recorded in a potential window from 200 mV to -600 mV at a rate of 1 mV s^{-1}. A series of rotation rates were used consistently in each test (500, 900, 1600, 2500, 3600 rpm).

Charge transfer resistances were calculated from the slope of the linear portion of the current-potential curve at low overpotential (c. ± 10 mV), recorded at 2500 rpm. Similar values were obtained using the 500 rpm data. Mass-transport corrected Tafel plots (not shown) were calculated using the 2500 rpm data for each sample. Exchange current densities were determined by extrapolating the Tafel slopes (at lower overpotential) to the potential at which the net current is zero, as determined form the linear part of the i-E curve.

Rotating Ring Disk Electrode (RRDE) Experiments were performed similarly on a Gamry Series G 750 Test System Bipotentiostat equipped with RDE710 Rotating Electrode. The collection efficiency of our system was determined to be 35% for both bare and catalyst-coated disk electrode surfaces. Collection efficiency was used to determine the adjusted ring current. This value was obtained using the ferrocyanide/ferricyanide system as described in the "User Manual for the Pine Modulated Speed Rotator" (see http://voltammetry.net/pine/rotating_electrode/theory). Briefly, the working electrode was obtained from Pine Research Instruments (E7R9 Series); the disk electrode (glassy carbon) potential was scanned from 350 mV to -500 mV at a rate of 2 mV s^{-1}, while the ring electrode (Au) potential was held at 500 mV (all potentials vs. Ag/AgCl). Experiments were conducted at a series of rotation rates (500, 900, 1600, 2500, 3000 rpm). The resulting data was processed using Kaleidagraph software.

For ORR studies, working RRDE electrodes were prepared by pipetting 12.6 µL of catalyst ink onto the GC disk surface (the amount deposited was scaled up to account for the increased disk electrode area of 0.2475 cm^2). Prior to deposition, the working electrode was carefully polished with alumina slurry, sonicated in de-ionized H_2O, and rinsed with ethanol. The counter was Pt° wire, and the reference electrode was Hg/HgO (0.1 M KOH). The potential of the disk electrode was scanned from 200 mV to -600 mV (vs. Hg/HgO) at a rate of 1 mV s^{-1}; the potential of the ring (area = 0.1866 cm^2) was held at 0.350 mV (vs. Hg/HgO). Experiments were conducted at a series of rotation rates from 500 to 3000 rpm in increments of 500 rpm. All experiments were conducted in 0.1 M KOH solution that had been purged with O_2 (for ORR data) or N_2 (for background measurements).

Methanol Poisoning Experiments: Chronoamperometric studies were performed using a VoltaLab potentiostat with RDE following a previously published procedure.[3] Specifically, 0.1 M KOH solution was purged with nitrogen for 20 minutes prior to the experiment. The RDE (prepared as previously described) was held at a potential of -250 mV (vs. Hg/HgO) for the duration of the experiment (t = 4000 seconds). From 0 to 2400 seconds, the solution remained under N_2-protection. At 2400 seconds, O_2 was introduced via gentle bubbling. At ~3400 seconds, 2% MeOH (w/w) was injected via micropipette. The solution remained under O_2 –protection for the remainder of the experiment. Holding potential for the experiment was -250 mV (vs. Hg/HgO). Rotation speed was 1000 rpm.

Conductivity Measurements

The conductivity of Vulcan, iRGO and GLC was measured on pressed pellets prepared by mixing 400 µL of 5% Nafion solution (Sigma Aldrich NAFION PERFLUORINATED ION-EXCHANGE POWDER, 5 WT % SOLUTION IN LOWER ALIPHATIC ALCOHOLS/H_2O) per 100 mg of the powdered carbon. The slurry was mixed and allowed to dry overnight. A 13 mm die

press (Carver) was filled with binder-coated carbon and pressed under 15,000 psi for 30 seconds. The resulting ~ 1 mm thick pellet was placed on a 4-wire NI PXI-4070 Signature conductivity meter and probed in multiple locations to find the average resistance.

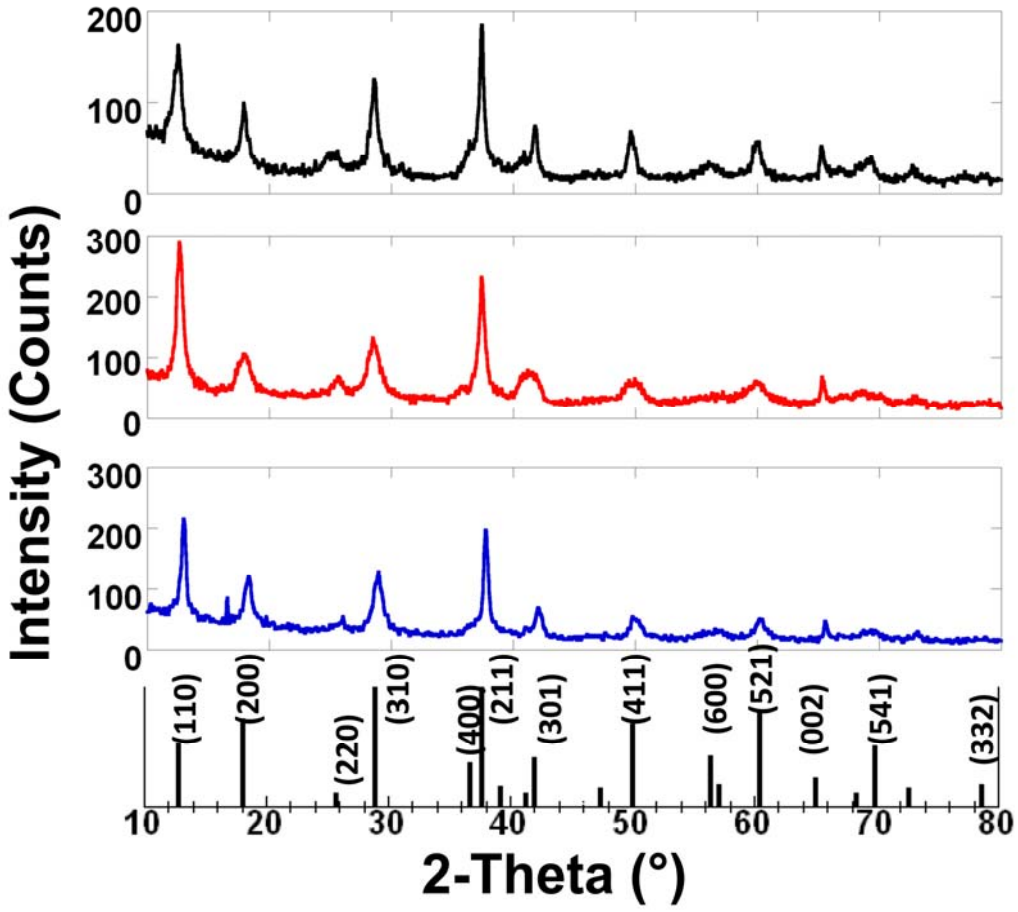

Figure S1. PXRD for (top) α-MnO_2, (middle) Ni-α-MnO_2 and (bottom) Cu-α-MnO_2 as indexed to JCPDS file no. 044-0141.

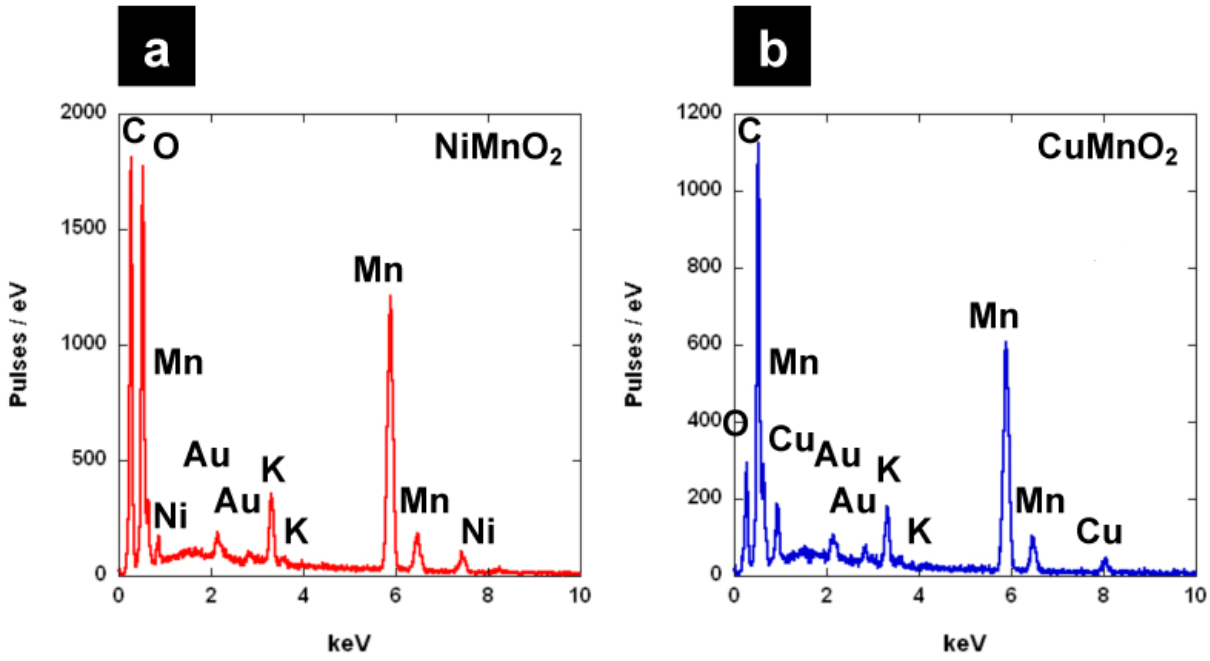

Figure S2. EDS spectra for a) Ni-α–MnO_2 , and b) Cu-α–MnO_2 nanowires.

HR-STEM data indicates that all nanowires are the α–MnO_2 phase. Each nanowire, as shown in the SEM in Figure 1, is an assembly of smaller wires. Doping with Cu or Ni does not change the lattice orientation. Each wire length is along the (002) orientation. EDS mapping indicates no high concentration regions of Cu or Ni indicating these cations are each distributed throughout the nanowire. Ni and Cu were found to be present at 10-12% and 10% (respectively) relative to Mn.

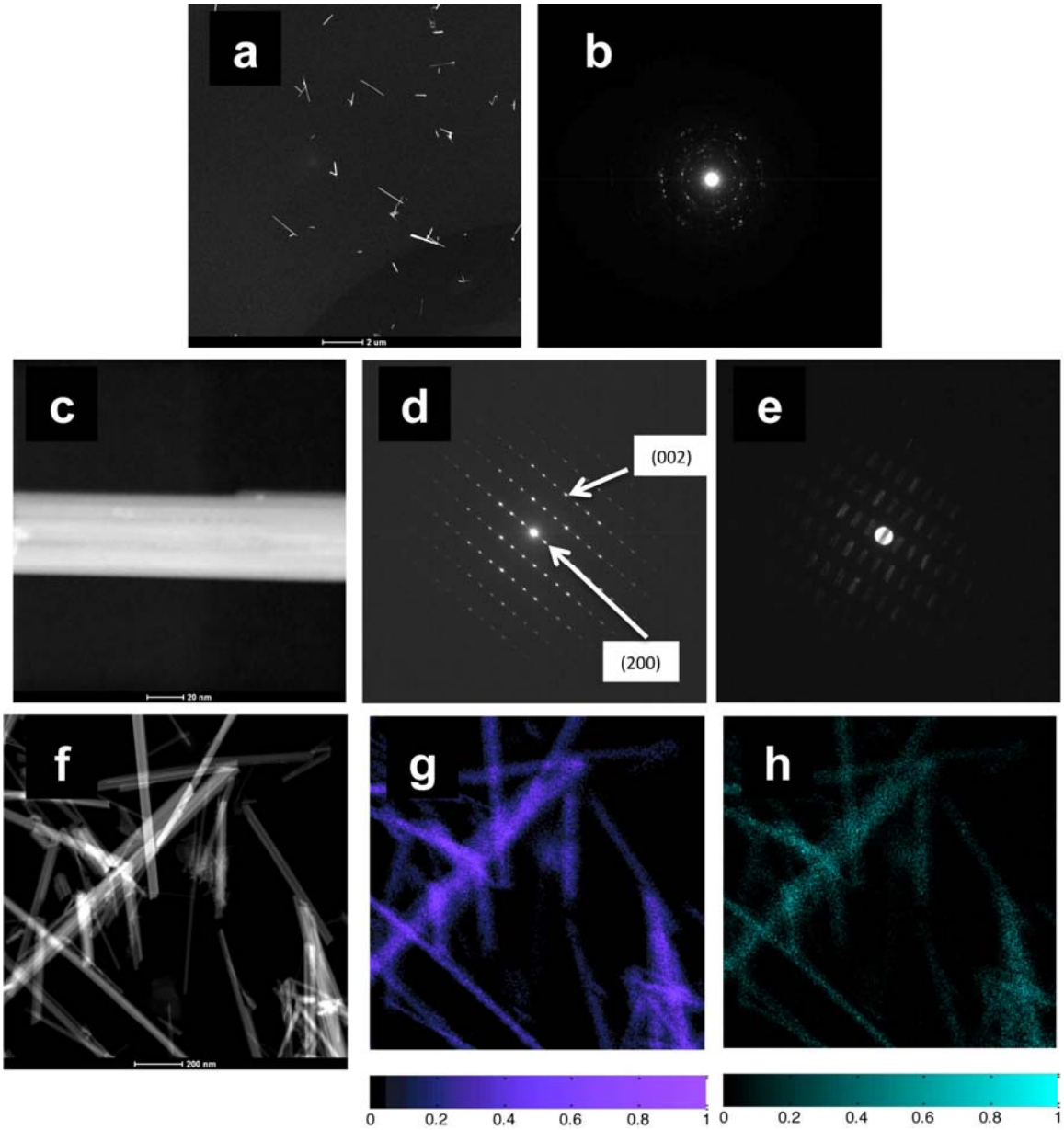

Figure S3. STEM, SAED and EDS mapping data for α–MnO_2 nanowires. a) Annular dark-field image, b) SAED on large field of view, c) individual nanowire, d) SAED on individual nanowire, e) out of focus SAED pattern showing the image of the nanowire (from d) and it's orientation relative to the lattice, f) Annular dark-field image at 1500 nm field of view, g) EDS Mn map, h) EDS K map.

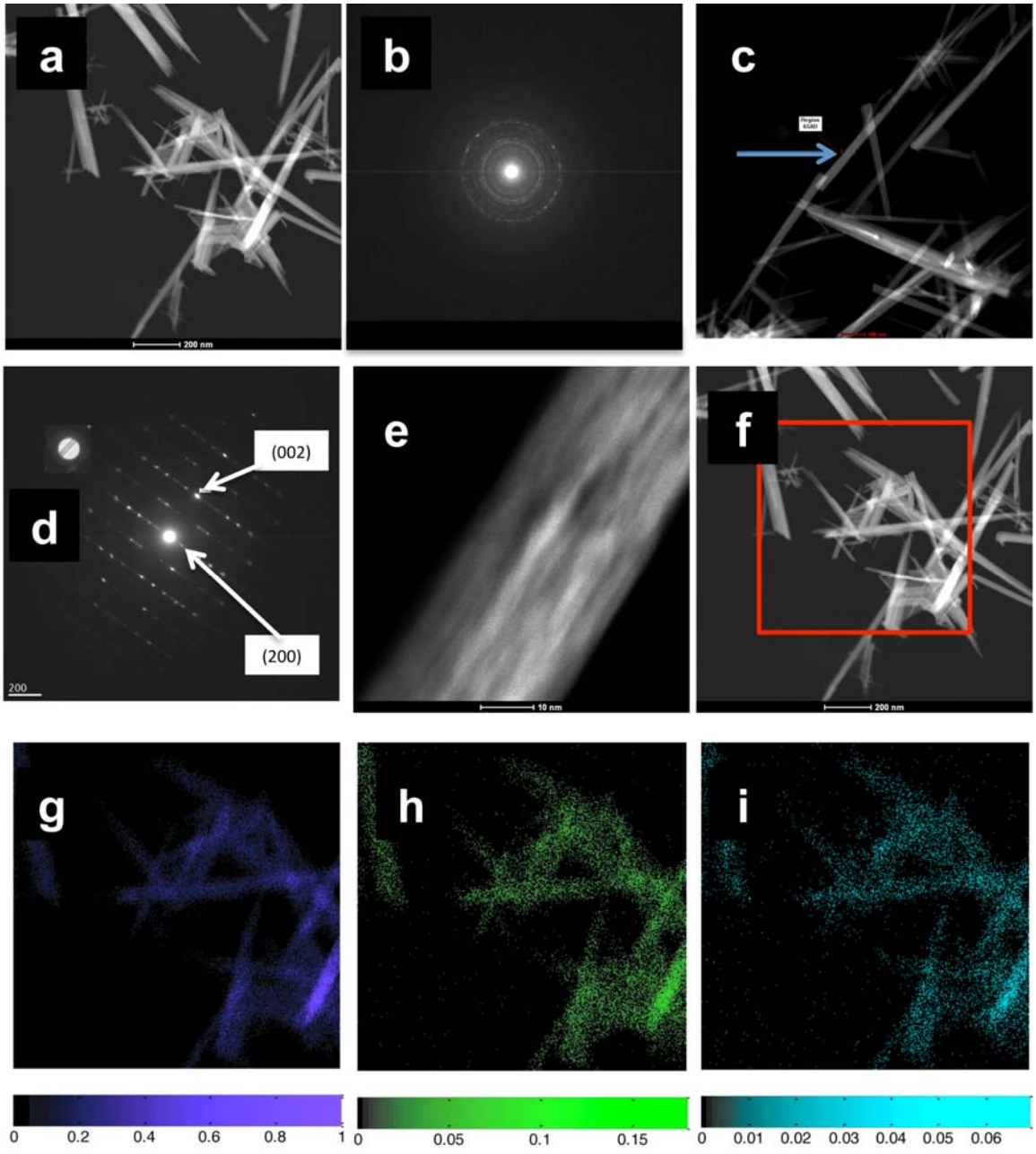

Figure S4. STEM, SAED and EDS mapping data for Ni-α–MnO_2 nanowires. a) Annular dark-field image, b) SAED on large field of view, c) individual nanowire, arrow indicates, d) SAED on individual nanowire as shown, e) high resolution image of nanowire, f) Annular dark-field image g) EDS Mn map at 900 nm field of view, h) EDS Ni map, i) EDS K map.

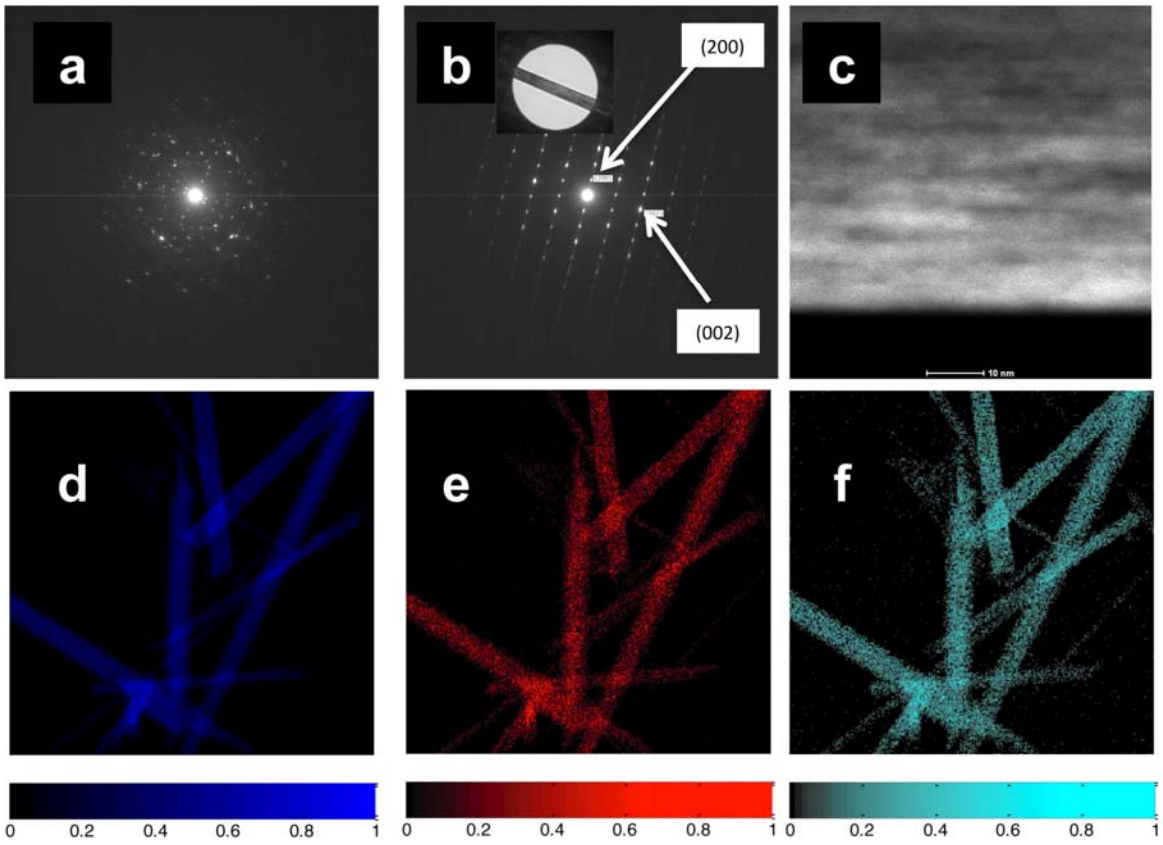

Figure S5. STEM, SAED and EDS mapping data for Cu-α–MnO_2 nanowires. a) SAED on large field of view, b) SAED on individual nanowire (as shown in inset), c) high resolution image of nanowire, d) EDS Mn map at 900 nm field, h) EDS Cu map, i) EDS K map.

.

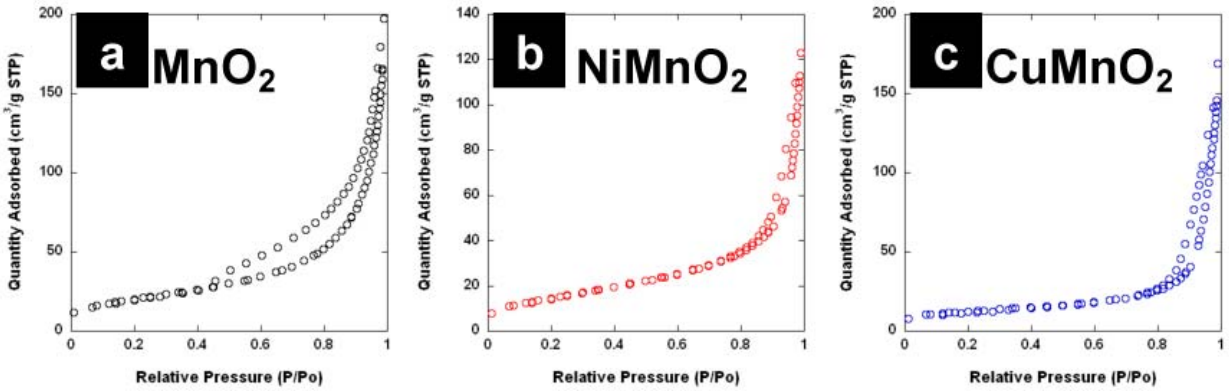

Figure S6. Nitrogen sorption isotherms (and BET surface areas) for a) α–MnO_2 (73.6 m^2/g), b) Ni-α–MnO_2 (54.1 m^2/g), and c) Cu-α–MnO_2 (43.7 m^2/g) nanowires.

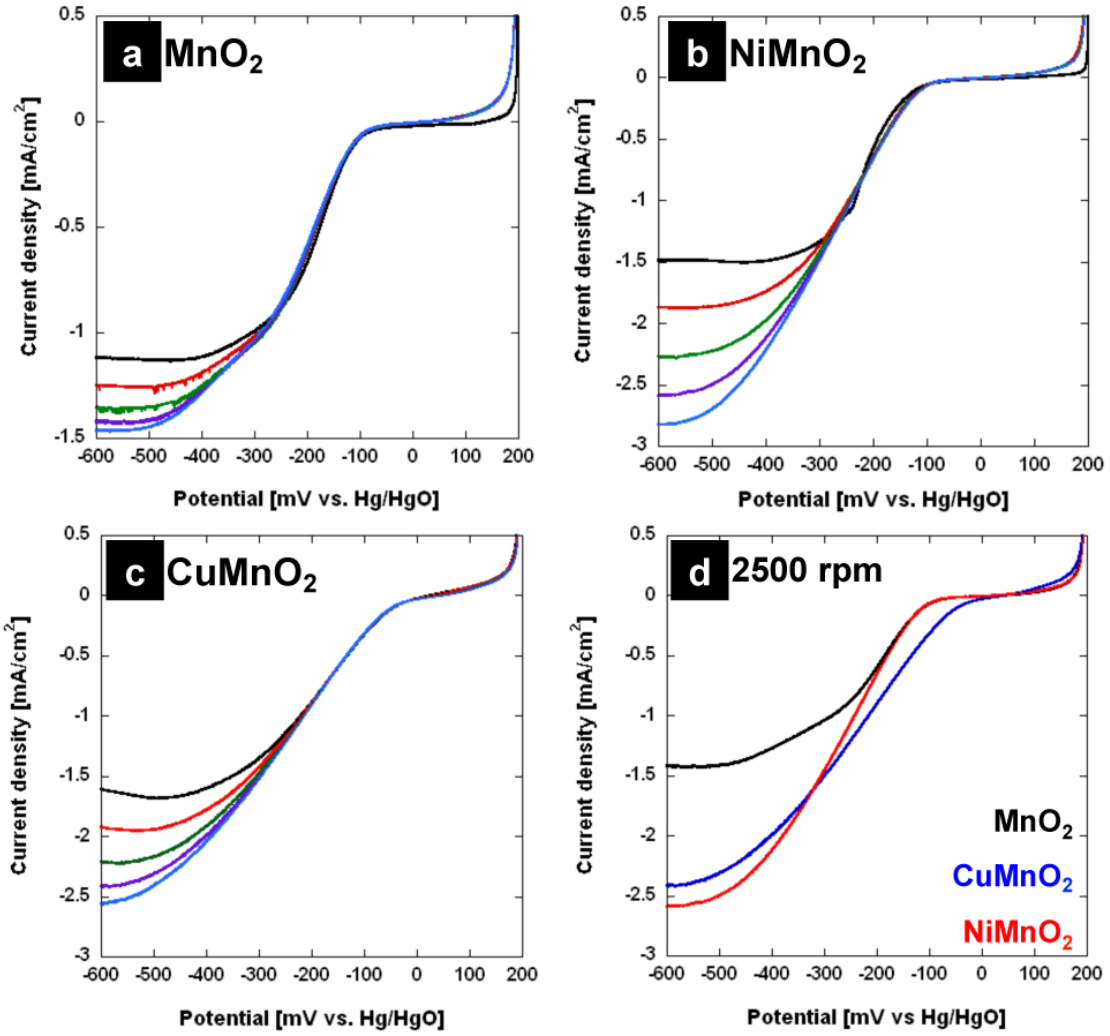

Figure S7: Linear scanning voltammograms for a) α–MnO_2, b) Ni-α–MnO_2, c) Cu-α–MnO_2 at 500, 900, 1600, 2500 and 3600 rpm, and d) a comparison of the three at 2500 rpm.

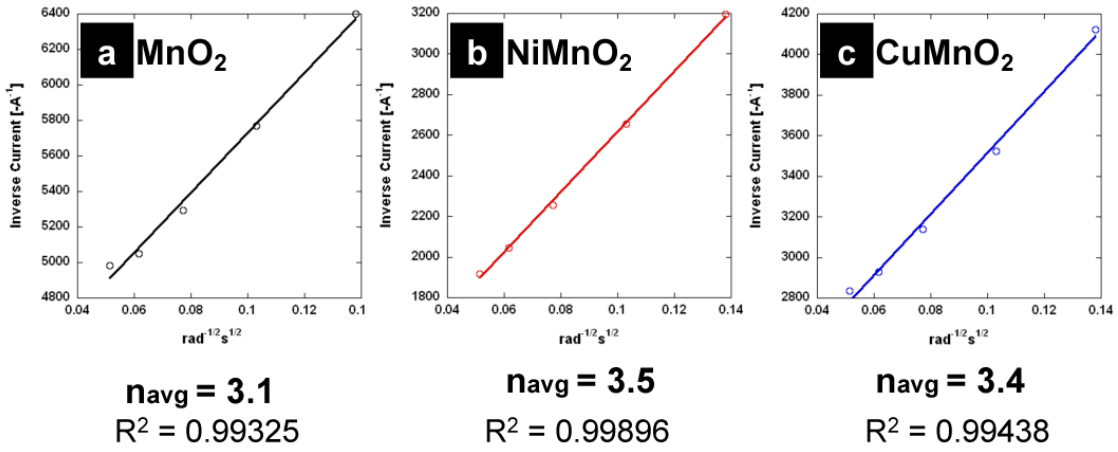

Figure S8: Koutecky-Levich Pots for a) α–MnO_2, b) Ni-α–MnO_2, and c) Cu-α–MnO_2.

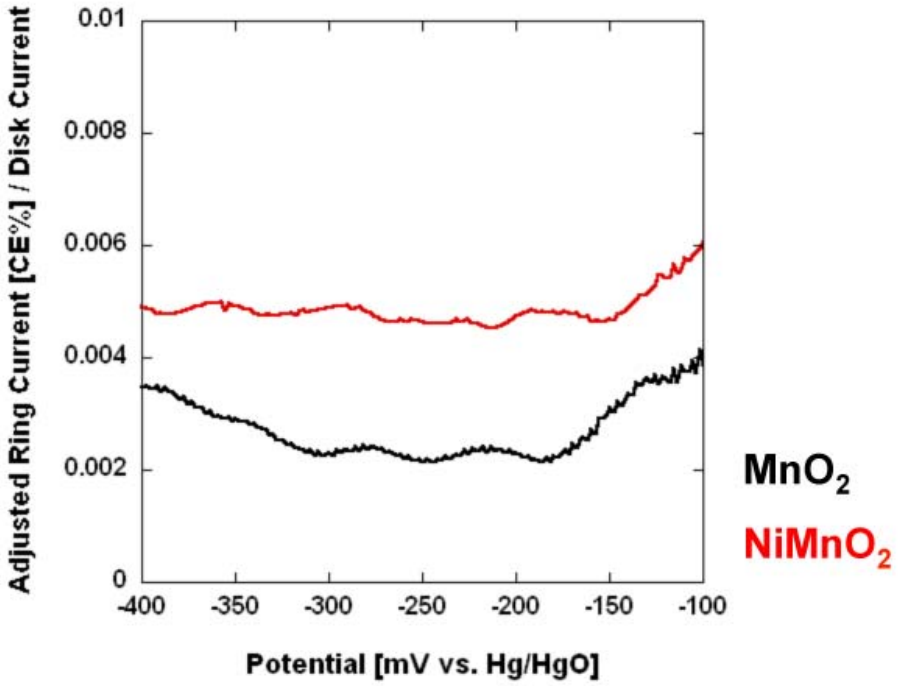

Figure S9: Comparison of peroxide production for α□MnO_2 and Ni-α□MnO_2 nanowires.

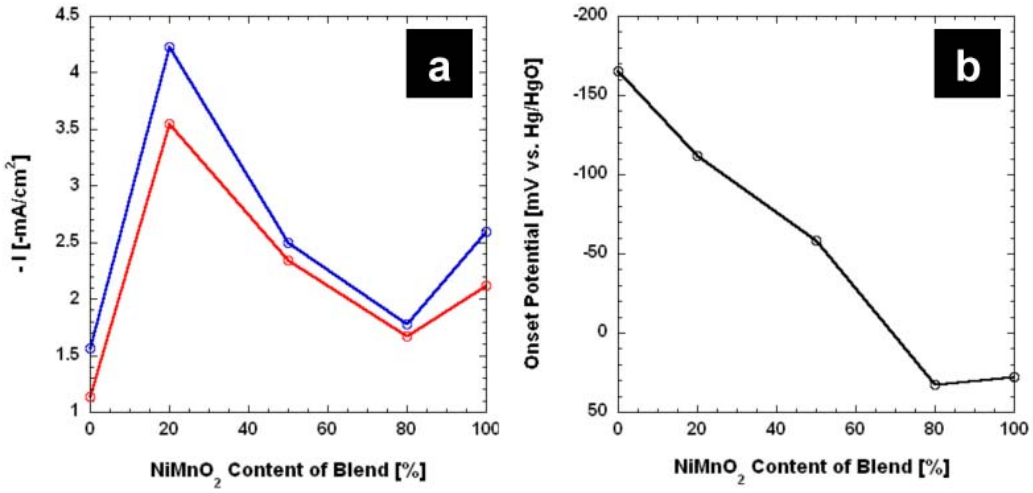

Figure S10: a) Steady state current (red = at -400 mV, blue = -600 mV) and b) onset values for varying composition of Ni-α□MnO_2/GLC blends at 2500 rpm.

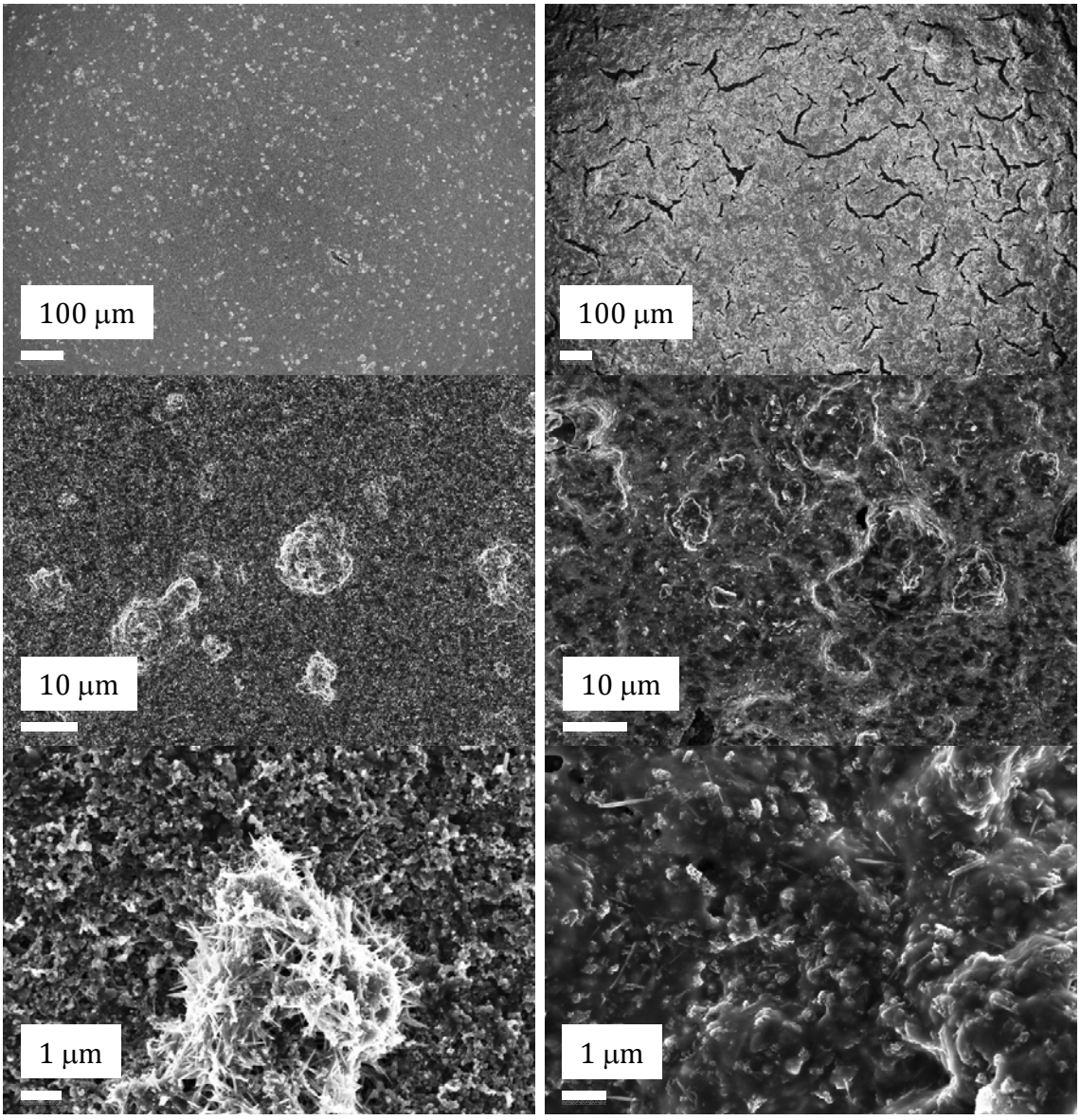

Figure S11: SEM images of increasing magnification for (left column) Vulcan/ $NiMnO_2$/binder and (right colum) GLC/$NiMnO_2$/binder: for Vulcan the majority of wires were found in the clustered/aggregated state while for GLC majority of the wires were dispersed throughout the carbon.

Images suggest that use of the higher surface area GLC leads to a better dispersion of the Ni-MnO_2 nanowires, which may also provide for the higher electro-catalytic activity observed with GLC as opposed to Vulcan.

Table S1. Four point probe conductivity measurements on pressed pellets of carbons. Data supports that increased activity with GLC is a result of the higher surface area and possibly better blending with the nanowires.

Resistance Values (Ω)	GLC	iRGO (DD479 053012)	Vulcan
	1.957	1.7	0.077
	3.381	1.99	0.094
	5.72	1.46	0.108
	2.36	2.71	0.064
	1.42	2.47	0.087
Average Resistance (Ω)	2.9676	2.066	0.086
Standard Deviation	1.697951796	0.520797465	0.016688319
Thickness (mm)	1.302	1.137	1.082
Thickness (cm)	0.1302	0.1137	0.1082
Resistance (Ω/cm)	22.79262673	18.17062445	0.794824399
Conductivity (S/cm)	2.588115498	4.257054578	107.4667928
Nafion (volume in total batch)	400 µL / 105 mg	200 µL / 52.7 mg	400 µL / 105.3 mg
Mass of Nafion in total batch (mg)	0.01748	0.00874	0.01748
Percent Nafion	0.016647619	0.01658444	0.01660019

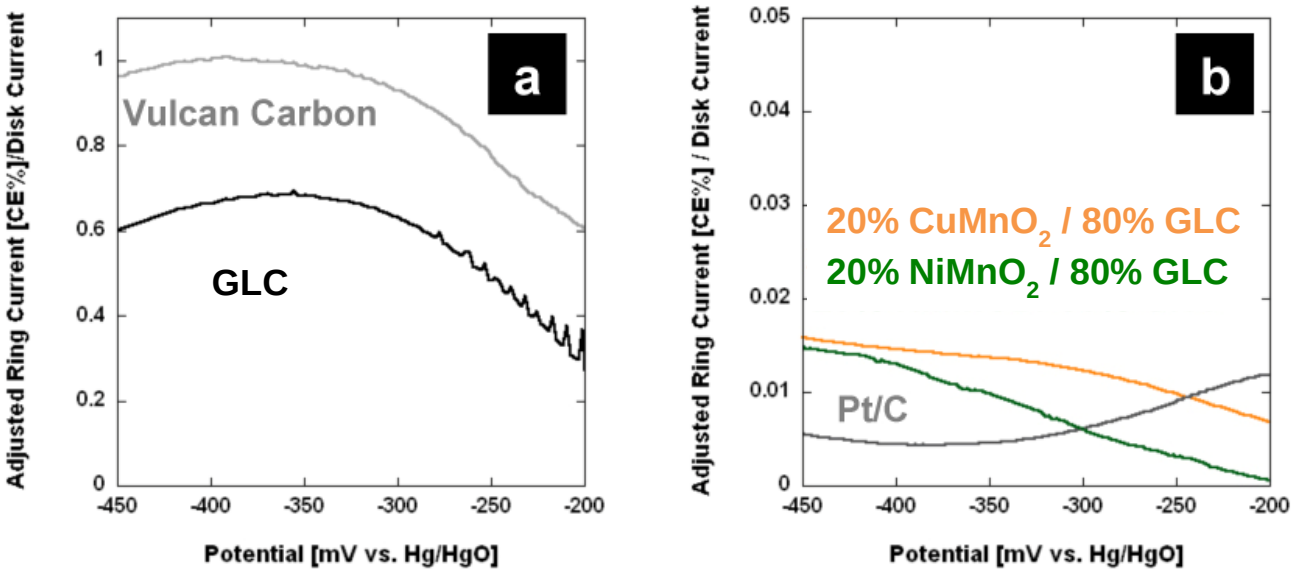

Figure S12: Comparison of peroxide production for a) Vulcan, GLC and b) 20% Cu-α□MnO_2/80% GLC, 20% Ni-α□MnO_2/80% GLC and 20% Pt/C.

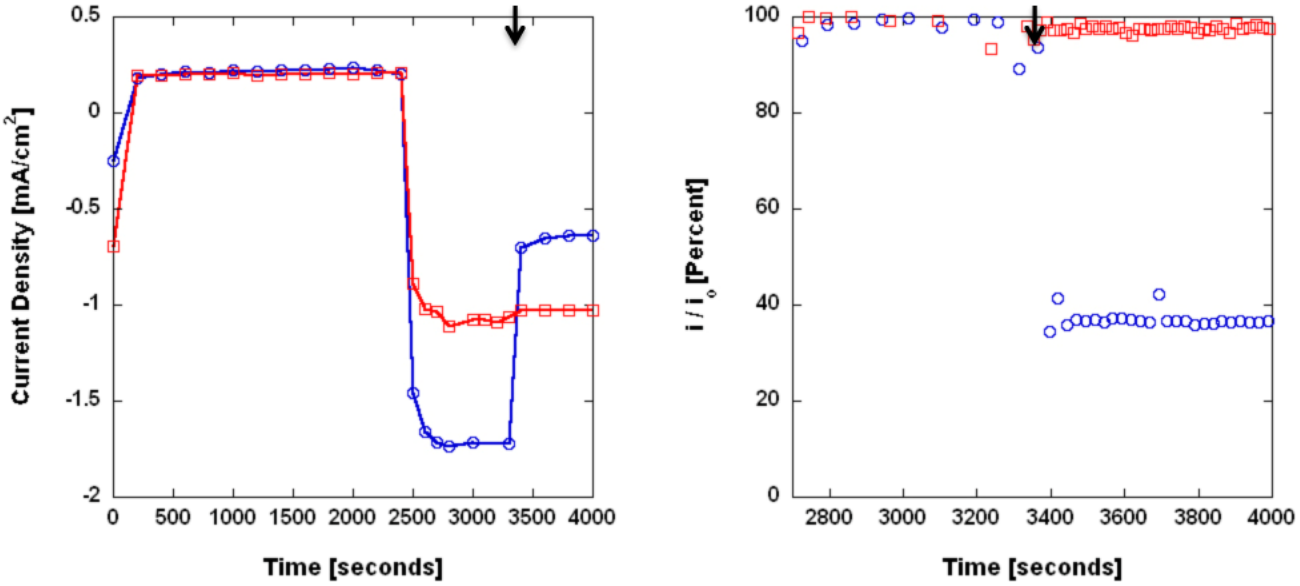

Figure S13: a) *i-t* chronoamperometric data obtained at 20% Pt/C (blue circles) and 20% $NiMnO_2$ / 80% GLC (red squares) electrodes at -250 mV (vs. Hg/HgO) at 1000 rpm in 0.1M KOH solution. b) Methanol poison effects on the current density of the electrode. Point of MeOH addition is indicated by the arrow.

The experiment[4] was performed as follows: The RDE (prepared as previously described) was held at a potential of -250 mV (vs. Hg/HgO) for the duration of the experiment (t = 4000 seconds). From 0 to 2400 seconds, the solution remained under N_2-protection. At 2400 seconds, O_2 was introduced via gentle bubbling. At ~3400 seconds, 2% MeOH (w/w) was injected via micropipette. The solution remained under O_2 –protection for the remainder of the experiment. Holding potential for the experiment was -250 mV (vs. Hg/HgO). Rotation speed was 1000 rpm.

.

References

1. F. Cheng, Y. Su, J. Liang, Z. Tao and J. Chen, *Chemistry of Materials*, 2010, **22**, 898-905.
2. F. Y. Cheng, J. Z. Zhao, W. Song, C. S. Li, H. Ma, J. Chen and P. W. Shen, *Inorg. Chem.*, 2006, **45**, 2038-2044.
3. K. Gong, F. Du, Z. Xia, M. Durstock and L. Dai, *Science*, 2009, **323**, 760-764.
4. L. Qu, Y. Liu, J.-B. Baek and L. Dai, *ACS Nano*, 2010, **4**, 1321-1326.